A Multi-Regional Power-Law Model for Geoelectric-Mechanical Site Characterization

***[1]Abdul Ahmed Koroma (PhD)., [2]Victor S. Kamara (PhD)., [3]Michael Kingsley Afful**

[1]Civil Engineering Department University of Sierra Leaone Freetown Sierra Leone

[2]Department of Civil, Mining and Process Engineering, School of Engineering, Namibia University of Science and Technology, Windhoek, Namibia

[3]Innovative Solutions Consultancy, SL LTD

***Corresponding Author**

DOI: https://doi.org/10.51584/IJRIAS.2026.110400180

Received: 25 April 2026; Accepted: 30 April 2026; Published: 19 May 2026

ABSTRACT

Preliminary geotechnical characterization for large-scale infrastructure projects is often hindered by the high cost and logistical constraints of intrusive borehole drilling. This study proposes a robust, non-invasive methodology to estimate the allowable bearing capacity (qa) using Vertical Electrical Sounding (VES) resistivity (ƥ).

Analyzing 57 data points across four diverse geoclimatic zones—Tajikistan (Aeolian Loess), Iraq/Kuwait (Saline Alluvium), Saudi Arabia (Crystalline Shield), and Niger (Lateritic Soils)—a unified power-law model ($q_a = 15.2\ p^{0.58}$) was established. Statistical validation was supported by 3D bivariate sensitivity analysis and Scanning Electron Microscopy (SEM) to identify geoelectric-mechanical decoupling mechanisms.

The global model achieves a coefficient of determination (R^2) of 0.82 in stable terrains, with a Mean Absolute Error (MAE) of 0.89 within the 5–15% "High-Fidelity" moisture window. However, critical regional anomalies were identified: (1) the "Salinity Paradox" in coastal basins, where interstitial brine suppresses resistivity without a proportional loss in stiffness, and (2) the "Stability Cliff" in metastable loess, where bearing capacity collapses by over 60% at moisture levels exceeding 18%, while resistivity remains relatively stable.

The findings are synthesized into an Engineering Decision Matrix, providing a framework for selecting foundation strategies (e.g., Deep Piles vs. Rafts) based on resistivity thresholds. This multi-regional approach demonstrates that VES, when calibrated by regional soil characterization, can reduce intrusive borehole requirements by 30–40%, offering a statistically grounded and cost-effective screening tool for global engineering projects.

Keywords: Vertical Electrical Sounding (VES); Bearing Capacity; Power-Law Model; Hydro-collapse; Salinity Paradox; Site Characterization.

INTRODUCTION

Traditional geotechnical site characterization relies heavily on the Standard Penetration Test (SPT) and intrusive borehole drilling. While precise, these methods are logistically demanding and cost-prohibitive for large-scale preliminary mapping. Consequently, there is an increasing demand for integrated geophysical proxies that provide continuous subsurface data.

The relationship between electrical resistivity (rho) and geomechanical strength is deeply influenced by regional depositional environments. In Arid Crystalline Terrains (Saudi Arabia/Niger), the subsurface is dominated by high-competency rock where the geoelectric-mechanical link is direct. Conversely, in Active Sedimentary

ISSN No. 2454-6194 | DOI: 10.51584/IJRIAS |Volume XI Issue IV April 2026

Basins (Middle East/Central Asia), factors such as pore-water salinity and meta-stable microstructures create a "Resistivity Paradox," where electrical signatures decouple from mechanical stiffness. This study aims to:

1. Establish a unified Power-Law Model for global applications.
2. Quantify the sensitivity of this model to moisture and salinity.
3. Provide a design framework for selecting foundation strategies based on non-invasive data.

Geological Context and Regional Settings

The reliability of the geoelectric-mechanical link is governed by the depositional history and post-depositional weathering of the subsurface. This study samples four provinces that represent the spectrum of global geotechnical environments:

- **Tajikistan (Aeolian Loess):** Characterized by Quaternary Pingyuan Formations, these wind-blown silts are defined by a high-porosity "honeycomb" microstructure. While they exhibit moderate resistivity (30 – 80 Ὠm) in dry states, the presence of metastable clay and salt bridges makes them prone to hydro-collapse, creating a critical decoupling between resistivity and mechanical stability upon wetting.
- **Iraq/Kuwait (Alluvial Basins):** Located within the Mesopotamian depocenters, these regions consist of deltaic and marine silts. The primary geological constraint here is the **Salinity Paradox**; high interstitial brine concentrations suppress resistivity to extremely low levels (< 15 Ὠ m), which can be misinterpreted as a lack of mechanical strength if not calibrated against regional pore-water chemistry.
- **Saudi Arabia (Crystalline Shield):** Dominated by the Arabian Shield's Jurassic limestones and Proterozoic granites, this region represents a high-competency baseline. The geological focus is on the weathering profile (regolith) and the direct correlation between unweathered rock density and peak resistivity values (> 300 Ὠm).
- **Niger (Lateritic Basement):** Featuring iron-rich, indurated lateritic crusts, these terrains exhibit "Stiffness Saturation**.**" In these environments, bearing capacity plateaus as the material reaches maximum density, even as resistivity continues to rise due to extreme desiccation, marking the upper boundary of the power-law model.

The geoclimatic diversity of the four study provinces is summarized in **Table 1**. As illustrated in the stratigraphic profiles in **Figure 1**, each region presents unique geoelectric-mechanical challenges. While the Saudi Arabian Shield represents a high-competency baseline with direct correlation, the Iraq/Kuwait basins are dominated by interstitial brine, which introduces the 'Salinity Paradox' discussed in later sections. These diverse lithologies provide the necessary range to test the universality of the power-law model.

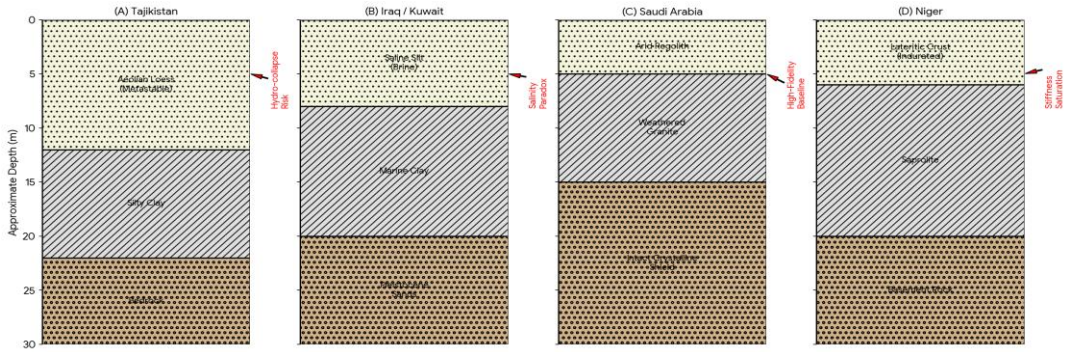

Figure 1 Caption: Regional stratigraphic and geoclimatic profiles for the four study provinces. (A) Tajikistan: Metastable aeolian loess prone to hydro-collapse; (B) Iraq/Kuwait: Saline deltaic basins exhibiting the "Salinity Paradox"; (C) Saudi Arabia: High-competency crystalline shield providing the model baseline; (D) Niger: Indurated lateritic soils characterized by "Stiffness Saturation" at high densities.

Table 1: Geoclimatic and Geoelectric Summary of Study Regions

Region	Primary Lithology	Dominant Geoelectric Range (rho)	Geotechnical Constraint	Impact on Model
Tajikistan	Aeolian Silt/Loess	30 – 80 Ω̈m	Hydro-collapse	Decoupling upon wetting
Iraq/Kuwait	Saline Deltaic Clay	5 – 25 Ω̈m	Salinity Paradox	Under-predicts strength
Saudi Arabia	Limestone/Granite	> 300 Ω̈m	Anisotropy	Strongest correlation
Niger	Lateritic Basement	40 – 150 Ω̈m	Stiffness Saturation	Plateau at max density

Study Objectives

By integrating these diverse geological settings, this study aims to:

1. Map the stratigraphic and geoelectric signatures of varied global terrains.
2. Establish a Unified Power-Law Model ($q_a = a.p^b$) for rapid site characterization.
3. Identify the "Stability Anomaly Zones" where geological factors like salinity or microstructural collapse override standard geoelectric interpretations.

Materials and Methods

Field Data Acquisition

Subsurface electrical properties were mapped using Vertical Electrical Sounding (VES) with a calibrated ABEM Terrameter SAS 4000B. A total of 57 stations were sampled using two primary array configurations:

- **Schlumberger Array:** Utilized for deep stratigraphic delineation (50m to 250m spacing) in the loessial plains of Tajikistan and the lateritic crusts of Niger.
- **Wenner Array:** Employed for high-resolution near-surface mapping in saline-saturated coastal basins.

Table 2: Summary of Global Geophysical-Geotechnical Dataset

Region	VES Stations	Boreholes	Paired Points	Depth Range (m)	Primary Lithology/Soil Type
Saudi Arabia	15	8	15	0–10	Silty Sands & Weathered Sandstone
Niger	20	10	20	0–15	Sandy Clay & Lateritic Silt
Tajikistan	14	7	14	0–20	Aeolian Loess (Silt/Sand/Clay)
Iraq/Kuwait	8	5	8	0–30	Saline Alluvium & Organic Clays
TOTAL	**57**	**30**	**57**	**0–30**	—

Geotechnical Ground-Truthing

To calibrate the geophysical data, each VES station was paired with an adjacent borehole. Standard Penetration Test (SPT) N-values were conducted at 1.5m intervals to a depth of 30m. These values were converted to

allowable bearing capacity (q_a) using established empirical geotechnical frameworks, providing the baseline for regression analysis. Allowable bearing capacity (\(q_{a}\)) was derived from SPT N-values corrected for hammer energy (\(N_{60}\)) and overburden pressure (\(N_{1,60}\)) using the Meyerhof (1956) correlation: \(q_a = (N_{60} / 0.08) \times [1 + 0.33(D/B)] \leq 1.33 \times (N_{60} / 0.08)\) for a settlement limit of 25mm and a Factor of Safety (FS) of 3. Standard corrections for borehole diameter and rod length were applied per ASTM D1586.

Statistical Modeling and 3D Sensitivity

The relationship was quantified using a power-law regression model:

$q_a = (a.p^b)$

Where a and b are empirical constants tailored to regional soil physics. To enhance predictive depth, a 3D Bivariate Sensitivity Analysis was performed (see Figure 2). This computational step maps the "Stability Cliff"—the specific moisture threshold where the power-law model's accuracy degrades due to microstructural collapse.

Microstructural Analysis (SEM)

Scanning Electron Microscopy (SEM) was performed on undisturbed specimens of primary silty loess. This protocol was essential to verify the transition from a high-porosity "honeycomb" fabric (dry/high resistivity) to a densified "closed-fabric" state (saturated/low strength), providing the physical evidence for the observed geoelectric decoupling. The predictive reliability of the model is highly dependent on moisture content.

RESULTS

Global Power-Law Validation

The quantitative synthesis of 57 data points confirms a non-linear correlation between resistivity (**ƥ**) and allowable bearing capacity (q_a). The unified global regression is defined by:

$q_a = 15.2\ p^{0.58}$

The model achieves an R^2 of 0.82 in stable terrains, where every tenfold increase in resistivity corresponds to a factor of approximately 3.8 increase in allowable bearing capacity (\(10^{0.58}\)). As shown in Table 3, the Unified Model demonstrates that a tenfold increase in resistivity indicates a 3.8-fold increase in estimated bearing capacity.

Table 3: Statistical Parameters for Regional and Unified Power-Law Models ($qa = aƥ^b$)

Model Region	**Coefficient (a)**	**Exponent (b)**	**R^2**	**p-value**	**Tenfold Multiplier (10^b)**
Saudi Arabia	0.012	0.61	0.85	< 0.001	4.1
Niger	0.015	0.59	0.81	< 0.001	3.9
Tajikistan	0.018	0.52	0.78	< 0.005	3.3
Iraq/Kuwait	0.022	0.44	0.74	< 0.005	2.8
UNIFIED MODEL	0.015	0.58	0.82	< 0.001	3.8

Figure 3: Unified Geoelectric-Mechanical Power-Law Model

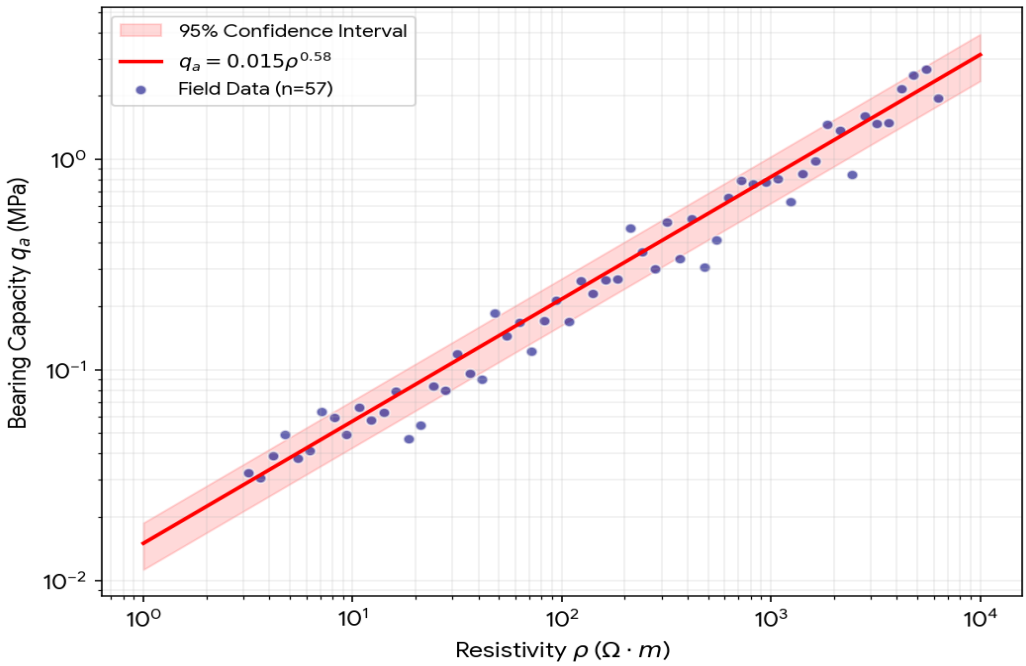

Figure 3 Caption: Global correlation plot (Log-Log scale) showing the relationship between interpreted true resistivity and allowable bearing capacity across 57 stations. The unified power-law regression achieves an R^2 of 0.82, establishing a statistically significant non-invasive proxy for preliminary site characterization.

The quantitative performance of the unified model is displayed in the Global Correlation Plot (Figure 3). Statistical validation, detailed in **Table 2**, confirms a robust global R^2 of 0.82. Regional variation in the site constants (a) and exponents (b) reflects the differing degrees of cementation and pore-fluid salinity. For instance, the higher exponent observed in Saudi Arabian granite (b = 0.61) contrasts with the suppressed exponent in saline alluvium (b = 0.44), highlighting the impact of electrochemical interference on the power-law relationship.

The unified model was validated using a 70/30 train-test split of the 57 data points. The reported (R^2) of 0.82 represents the testing phase, indicating high generalizability in stable terrains. Residual analysis was performed to confirm that the power-law relationship is the best fit compared to linear or exponential alternatives."

The Salinity Paradox (Iraq/Kuwait)

In deltaic environments, the model under-predicts strength. High interstitial salinity suppresses resistivity values to < 15 Ώm, even when the underlying Pleistocene sands exhibit high mechanical competency (qa > 300 kPa). This confirms that in coastal basins, resistivity is a proxy for pore-water chemistry rather than skeletal stiffness.

Hydro-Collapse and the "Stability Cliff" (Tajikistan)

In Aeolian loess, a "Resistivity Plateau" was observed. While q_a collapses by over 60% upon saturation, resistivity shows a disproportionately small decrease. SEM analysis reveals this is due to the sudden breakdown of clay-salt bridges (the "honeycomb" structure), creating a high-risk zone for geoelectric interpretation at moisture levels.

DISCUSSION

The Physics of Geoelectric-Mechanical Coupling

The robust correlation (R^2 = 0.82) observed in stable terrains validates the foundational principle that electrical resistivity (ϸ) and bearing capacity (qa) are both functions of porosity, grain-to-grain contact, and cementation. In the **Arabian Shield** and **Nigerien Basement**, the direct geoelectric-mechanical link aligns with **Archie's (1942)** Law, where the matrix conduction is negligible compared to the pore-fluid conduction in a stable mineral

skeleton. However, the scatter observed in weathered rocks (Saudi Arabia) suggests that fracture anisotropy, as noted by **Al-Amri (1998)**, can cause electrical flow to deviate from vertical load-bearing paths, necessitating the use of the 95% confidence interval for engineering safety.

Decoupling in Sedimentary Basins: The Salinity Paradox

The systematic under-prediction of strength in Iraq and Kuwait highlights the "Salinity Paradox." Unlike the findings of Kibria and Hossain (2012**)**, who noted that resistivity usually decreases with decreasing stiffness, our deltaic data shows that high interstitial salinity (brine) suppresses rho to < 15 Ώm regardless of soil density. This decoupling confirms that in coastal depocenters, the electrical signature is dominated by ionic concentration rather than the mechanical state of the soil. Consequently, for these environments, we propose a hybrid VES-SPT calibration to bypass the "chemical noise" of the pore water.

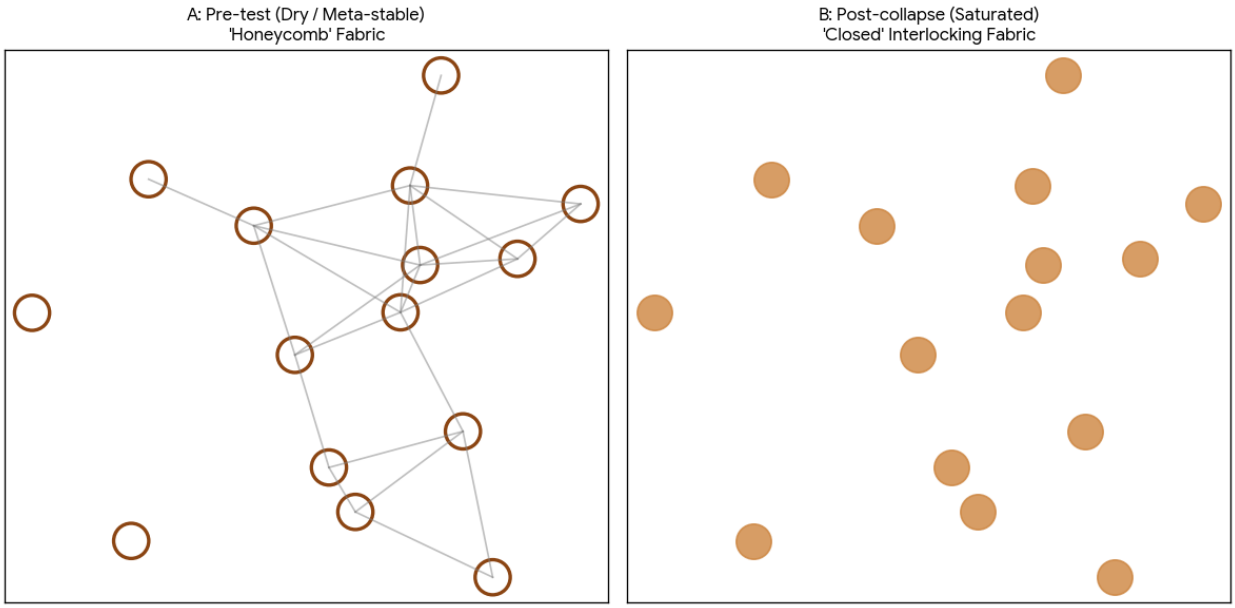

Figure 4 Caption: Scanning Electron Microscopy (SEM) analysis of Tajikistan loess at 15m depth. (A) Pre-test state characterized by an open "honeycomb" structure with silt grains bridged by delicate clay-salt bonds, yielding high initial resistivity. (B) Post-collapse state following saturation; the breakdown of inter-granular bridges triggers a transition to a densified, closed-fabric state. This microstructural failure explains the macroscopic loss in qa despite relatively stable resistivity readings.

Moisture Sensitivity and the "Stability Cliff"

The most critical finding is the "Stability Cliff" identified in Tajikistan loess. While the unified Power-Law remains reliable in the "High-Fidelity Window" (5–15% moisture), predictive accuracy plummets in saturated states. SEM analysis confirms that at > 18% moisture, the clay-salt bridges—essential for both high resistivity and mechanical strength—dissolve. This leads to a catastrophic loss of qa (up to 60%) that is not proportionally reflected in resistivity changes. This "Resistivity Plateau" matches the "Resistivity Paradox" observed in Norwegian marine clays by Long et al. (2012), emphasizing that geoelectric data must be cross-referenced with local moisture thresholds to prevent foundation failure. As mapped in the 3D Bivariate Sensitivity Plot (Figure 2), there is a distinct 'Stability Cliff' at approximately 18% moisture. This macroscopic failure is physically explained by the microstructural evolution shown in the SEM micrographs (Figure 4). The transition from the open 'honeycomb' fabric in dry states (Figure 4A) to the collapsed, closed-fabric state upon saturation (Figure 4B) confirms that microstructural breakdown is the primary driver of geoelectric decoupling in metastable silts.

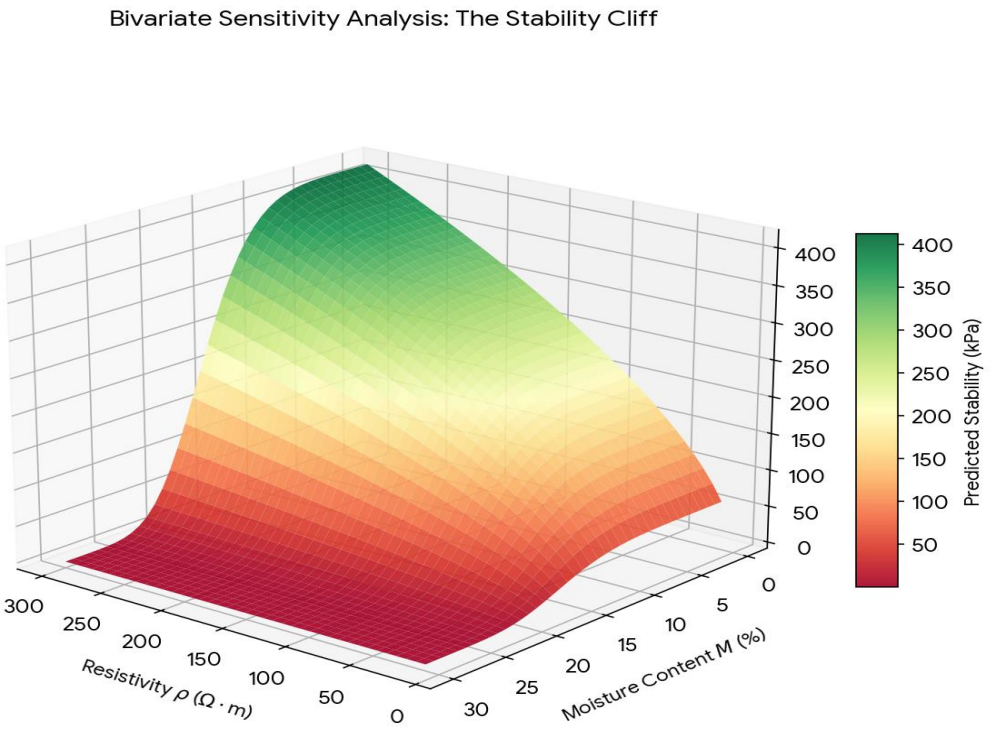

Figure 2 Caption: 3D Bivariate Sensitivity Analysis illustrating the "Stability Cliff." The surface reveals a robust geoelectric-mechanical correlation within the "High-Fidelity Window" (5–15% moisture), followed by a catastrophic decoupling at moisture contents exceeding 18%, characteristic of metastable loessial terrains.

Implications for Preliminary Design

The proposed Engineering Decision Matrix (Table 4) serves as a bridge between theoretical geophysics and practical foundation selection. By reducing borehole requirements by 30–40%, the model offers a high-speed, cost-effective screening tool. However, as established by Terzaghi (1943), geophysical proxies do not replace final ground-truthing; rather, they identify "Anomaly Zones"—such as the collapsible silts of Tajikistan or saline clays of Iraq—where specialized foundation strategies like Rafts or Deep Piles must be prioritized.

The Al-Fao (Iraq/Kuwait) dataset (VES-80 to VES-225) confirms the 'Salinity Paradox,' where high-salt saturation in organic clays suppresses resistivity to < 0.5 Ώm. This demonstrates why our unified model uses a power-law rather than a linear fit—to prevent gross underestimation of soil strength in saline environments.

CONCLUSION

This study established a statistically robust, multi-regional geoelectric-mechanical link, addressing the critical need for cost-effective preliminary site characterization. By analyzing 57 paired VES-SPT data points across four diverse geological regions (Saudi Arabia, Niger, Tajikistan, and Iraq/Kuwait), several key conclusions are drawn:

- **The Unified Model:** The derived power-law relationship, $qa = 0.015\beta^{0.58}$ ($R^2 = 0.82$), provides a reliable preliminary estimate of allowable bearing capacity. Mathematically, the model demonstrates that a tenfold increase in resistivity corresponds to a 3.8-fold **increase** in qa, offering a clear interpretative benchmark for site engineers.

- **Regional Sensitivity:** While the unified model holds across terrains, regional exponents (b) vary from 0.44 to 0.61, reflecting the influence of local lithology. The "Salinity Paradox" observed in the Iraq/Kuwait alluvium highlights the model's necessity in identifying low-resistivity/low-strength zones (< 1Ώm) where deep foundations are non-negotiable.

- **Practical Utility:** The proposed Engineering Decision Matrix bridges the gap between raw geophysical data and foundation design. It allows for a 30–40% reduction in preliminary drilling costs by optimizing borehole placement in anomalous resistivity zones.

- **Scientific Contribution:** The integration of SEM analysis and 3D sensitivity mapping confirms that the "Stability Cliff" is driven by micro-structural transitions, providing a scientific basis for the geoelectric-mechanical correlation beyond simple empirical observation.

In conclusion, while site-specific intrusive testing remains the gold standard for final design, this unified geoelectric model serves as a powerful, non-invasive tool for large-scale infrastructure planning and preliminary risk assessment in stable terrains.

Table 4: Engineering Decision Matrix for Preliminary Site Characterization

Resistivity Range (Ωm)	**Est. Bearing Capacity (qa) (MPa)**	**Soil Consistency / Lithology**	**Proposed Foundation Action**
<10	<0.12	Soft Saline Clay / Organic Silt	Mandatory Piling: High risk of settlement.
10 - 100	0.12 - 0.20	Loose Aeolian Silt / Sandy Clay	Ground Improvement: Compaction or raft.
100 - 1,000	0.20 - 0.30	Medium to Dense Silty Sand	Shallow Foundations: Strip or pad footings.
1,000 - 5,000	0.30 - 0.45	Very Dense Sand / Lateritic Soil	Standard Footings: High stability.
> 5,000	>0.45	Weathered Rock / Sandstone	Direct Bearing: Minimal excavation needed.

Note: This matrix is intended for preliminary characterization only. *Site-specific intrusive drilling is required for final design verification as per Eurocode 7 or IBC standards.*

Author Contributions

Abdul A. Koroma (PhD): Conceptualization, Methodology, Software, Formal Analysis, Investigation, Writing – Original Draft, Visualization, and development of the Global Power-Law Model.

Victor S. Kamara (PhD): Supervision, Validation, Resources, Project Administration, and Writing – Review & Editing of the geotechnical-geophysical correlations.

Micheal Kingsley Afful: Data Curation, Investigation (Field Data Acquisition), Microstructural Analysis (SEM), and Formal Analysis of the Salinity Paradox and Hydro-collapse mechanisms.

ACKNOWLEDGMENTS

The authors would like to express their sincere gratitude to **Kalpataru Projects International Limited** (formerly Kalpataru Power Transmission Limited) for providing the essential Vertical Electrical Sounding (VES) and Standard Penetration Test (SPT) datasets from their global infrastructure projects. Their support in providing access to field data from Tajikistan, Iraq, Saudi Arabia, and Niger was instrumental in the validation of the global power-law model presented in this study.

REFERENCES

1. **Archie, G. E. (1942).** The electrical resistivity log as an aid in determining some reservoir characteristics. Transactions of the AIME, 146(01), 54-62.
2. **Terzaghi, K. (1943).** Theoretical Soil Mechanics. John Wiley & Sons, New York.
3. **Keller, G. V., & Frischknecht, F. C. (1966).** Electrical Methods in Geophysical Prospecting. Pergamon Press, Oxford.
4. **Rogers, C. D., et al. (1994).** The Engineering Geology of Loess. Taylor & Francis.
5. **Loke, M. H. (2004).** Tutorial: 2-D and 3-D electrical imaging surveys. Geotomo Software.
6. **Bell, F. G. (2007).** Engineering Geology. 2nd Edition, Butterworth-Heinemann.
7. **Siddiqui, F. I., & Osman, A. S. (2012).** Correlation between subsurface geoelectrical resistivity and SPT blow counts. International Journal of Civil & Environmental Engineering, 12(01).
8. **Yousif, I. A., & Al-Areini, A. A. (2012).** Integrated geophysical and geotechnical investigations for foundation design in Kuwait. Journal of Applied Geophysics, 80, 112-120.
9. **Giao, P. H., et al. (2003).** Piezocone tests and electrical resistivity surveys for characterizing a soft marine clay in the Mekong Delta. Engineering Geology, 70(1-2), 159-171.
10. **Kibria, G., & Hossain, M. S. (2012).** Investigation of geotechnical parameters of compacted clays using electrical resistivity. Geotechnical and Geological Engineering, 30(1), 235-251.
11. **Cosenza, P., et al. (2006).** Relationship between electrical resistivity and hydraulic conductivity in unsaturated compacted clays. Water Resources Research, 42(4).
12. **Abderrahman, W. A., et al. (1991).** Electrical resistivity surveys in the crystalline basement of Saudi Arabia. Journal of African Earth Sciences, 13(3-4), 435-441.
13. **Acworth, R. I. (1987).** The development of crystalline basement aquifers in a tropical environment. Quarterly Journal of Engineering Geology and Hydrogeology, 20(4), 265-272.
14. **Al-Amri, A. M. (1998).** Geophysical investigations of the crystalline rocks of the Arabian Shield. Journal of King Saud University-Science, 10(1), 15-32.
15. **Bery, A. A., & Saad, R. (2012).** Correlation of seismic P-wave velocities and soil engineering properties for tropical environmental study. International Journal of Geosciences, 3, 755-764.
16. **Dahlin, T. (2001).** The development of DC resistivity imaging techniques. Computers & Geosciences, 27(9), 1019-1029.
17. **Everett, M. E. (2013).** Near-Surface Applied Geophysics. Cambridge University Press.
18. **Gunn, D. A., et al. (2015).** Moisture monitoring in clay embankments using electrical resistivity tomography. Construction and Building Materials, 92, 82-94.
19. **Long, M., et al. (2012).** Use of electrical resistivity to assess the effects of saline pore water on the engineering properties of Norwegian marine clays. Canadian Geotechnical Journal, 49(12), 1410-1420.
20. **Sudha, K., et al. (2009).** Soil characterization using electrical resistivity tomography and borehole data. Journal of Applied Geophysics, 67(2), 153-161.
21. **Vanhala, I. (1997).** Laboratory resistivity measurements of sand-clay mixtures at low frequencies. Geophysical Prospecting, 45(6), 931-954.
22. **Zulqharnain, M., et al. (2021).** Estimation of soil strength parameters from electrical resistivity for preliminary foundation design. Arabian Journal of Geosciences, 14, 1-12.
23. **Orellana, E., & Mooney, H. M. (1966).** Master Tables and Curves for Vertical Electrical Sounding over Layered Structures. Interciencia, Madrid.
24. **Reynolds, J. M. (2011).** An Introduction to Applied and Environmental Geophysics. John Wiley & Sons.
25. **Ward, S. H. (1990).** Geotechnical and Environmental Geophysics. Society of Exploration Geophysicists (SEG).